RESEARCH ARTICLE

ADVANCED MATERIALS INTERFACES Open Access

www.advmatinterfaces.de

Ultra-High-Throughput Nanoliter-Scale Liquid-Liquid Extractions and Reaction Mixture Purification

*Michelle J. Iwohn, Janne J. Wiedmann, and Pavel A. Levkin**

Miniaturizing chemical processes to the nanoliter scale is essential for reducing costs, increasing throughput, and enabling massively parallel experimentation with tens of thousands of samples. However, purification at this scale remains a major issue. Conventional methods like liquid-liquid extraction (LLE) are not applicable at nanoliter volumes without expensive and complex instrumentation, and even then, not at such extreme throughput. The droplet microarray (DMA) platform enables high-throughput synthesis in nanoliter droplets confined to hydrophilic spots on a superhydrophobic surface. Yet, purification of compounds at this small scale and high throughput remains challenging. Here, a novel approach is presented for parallel purification of thousands of microliter- to nanoliter-sized droplets via LLE. The method exploits the ability of hydrophilic spots to retain aqueous droplets under both air and organic solvents. By immersing the entire DMA into an organic solvent, all droplets simultaneously contact the organic phase, enabling rapid, parallel, single-step extraction across the entire array. This process eliminates the need for individual pipetting or complex phase separation equipment, making it scalable, cost-effective, and compatible with miniaturized, ultra-high-throughput workflows down to 15 nL volume and up to tens of thousands of parallel extractions.

1. Introduction

Miniaturization and parallelization of chemical processes are rapidly transforming the way modern science approaches compound screening, synthesis, and diagnostics.[1–3] Reducing reaction volumes to the nanoliter scale not only decreases reagent consumption and cost, but also enables massive throughput, facilitating the simultaneous performance of thousands or even hundreds of thousands of reactions.[4–7] These benefits over conventional bulk approaches are especially important in early-stage drug discovery (EDD), materials screening, and systems chemistry.[8–10] Despite its promise, miniaturization remains limited by several factors like a lack of all-purpose, high-throughput (HT) compatible methods and applicability over multiple scientific fields.[1,11–13] While many methods enable either parallel, high-throughput chemical synthesis or biological readout, only a few allow the combination of both on the same platform.[12–13] Additionally, a few platforms allow chemical work-up or purification at the same scale and throughput.[14] Most techniques for compound handling in such small scales rely on droplet-by-droplet manipulation using expensive equipment like robotic pipetting, acoustic dispensing or microfluidics (MF).[15]

The droplet microarray (DMA) platform allows the formation of thousands of individual droplets in the microliter- to nanoliter range on hydrophilic spots separated by superhydrophobic borders.[16–17] It supports massively parallel miniaturized workflows for chemical and biological applications and has been applied in diverse contexts, including live-cell screening, combinatorial synthesis, and digital bioassays.[16,18–21] However, purification of chemical synthesis remains an issue. Solid-phase synthesis (SPS) methods are one approach to overcome this problem and have helped to synthesize large and diverse compound libraries.[7,22] However, SPS is limited to specific reaction types, while solution-based synthesis (SBS) offers an almost unrestrained applicability.[23–25] Several strategies have been reported for introducing reagents into droplet arrays or transferring products between two immiscible phases. Surface nanodroplets formed by solvent exchange have been widely reported for ultrafast nanoextraction, chemical reactions, and colorimetric analysis.[26–28] The high surface-to-volume ratio enables fast analyte transfer, and applications like trace sensing, nanoextractions, integrated reaction and detection workflows.[27–30] However, such systems typically

M. J. Iwohn, J. J. Wiedmann, P. A. Levkin
Institute of Biological and Chemical Systems – Functional Molecular Systems
Karlsruhe Institute of Technology
Hermann-von-Helmholtz-Platz 1, 76344 Eggenstein-Leopoldshafen, Germany
E-mail: levkin@kit.edu
P. A. Levkin
Institute of Organic Chemistry
Karlsruhe Institute of Technology
Fritz-Haber-Weg 6, 76131 Karlsruhe, Germany

The ORCID identification number(s) for the author(s) of this article can be found under https://doi.org/10.1002/admi.202500465

DOI: 10.1002/admi.202500465

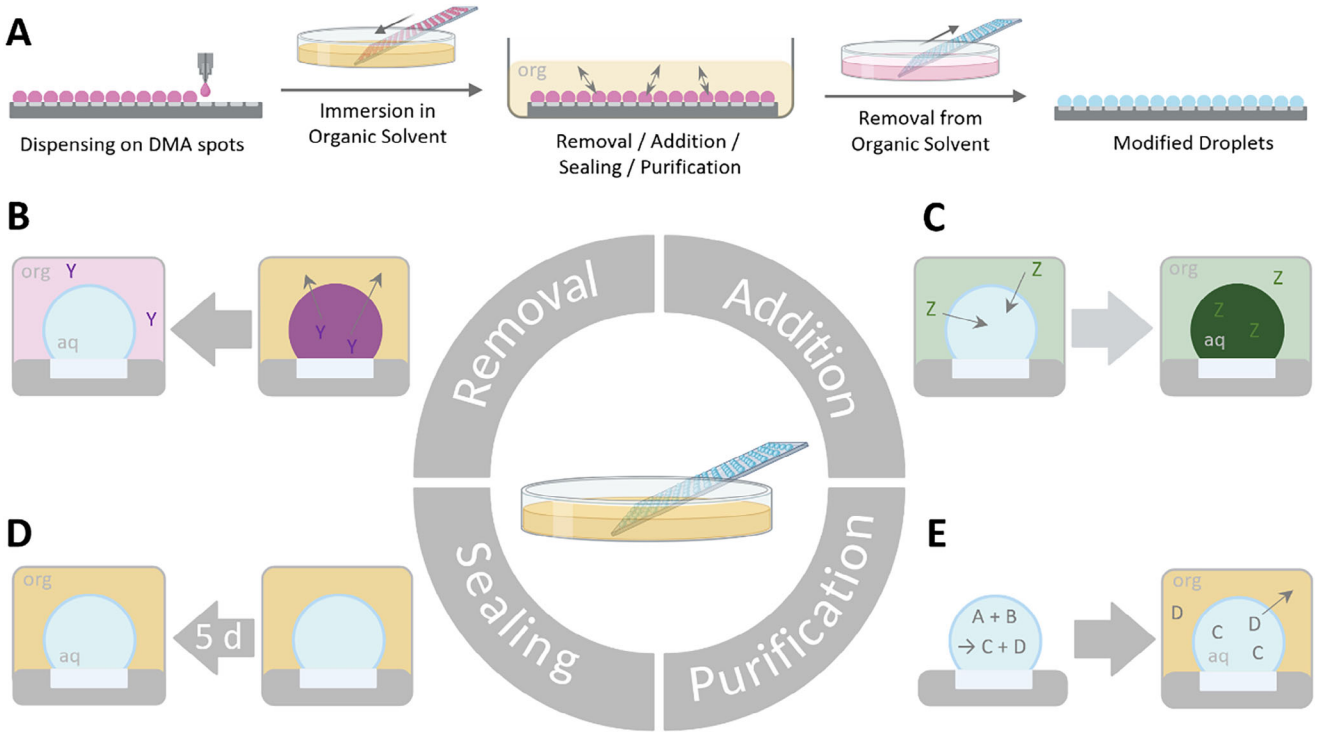

Figure 1. Dip-extraction method for parallel ultra-high-throughput droplet handling and treatment on the aqueous-organic-interphase using DMA as a platform. A) General workflow of the method. Aqueous droplets containing the desired additives are dispensed on the hydrophilic spots of a droplet microarray. The complete slide is immersed in a suitable organic solvent with or without additives, what enables the exchange of substances between the two phases. After removing the droplet microarray from the organic solvent, the droplets are still intact and feature the intended modification. In this work, we present four different applications for this system. B) Liquid-liquid extraction to remove a substance from the aqueous droplets. C) Liquid-liquid extraction to add a substance to the aqueous droplets. D) Prevent evaporation of the aqueous droplets by keeping them under an organic solvent. E) Perform a chemical reaction in the aqueous droplets and purify the product by extraction with dichloromethane.

require MF flow control and precise solvent exchange conditions, and the extremely small droplet volumes, typically in the femtoliter to low nanoliter range, limit their use in workflows requiring multi-step synthesis or downstream analysis. Sandwiching methods, as described by Benz et al. (2019), rely on physical contact between the droplets on a donor and a receiver DMA slide, enabling fast and direct compound transfer but requiring precise alignment and risking droplet deformation due to the applied physical force to merge the droplets vertically.[19] Wiedmann et al. (2023) introduced a method based on merging two neighbored, immiscible droplets on the same DMA slide for sample purification.[31] This method simplifies the handling but relies on a precise liquid dispenser for accurate droplet placement and merging. Based on the handling and precision difficulties described, both methods are limited in minimum droplet volume of ≈5 µL for Benz' approach and 100 nL for Wiedmann's strategy and therefore also in throughput. Although all methods are highly beneficial regarding the time and cost consumption compared to bulk methods, a new purification method that can be applied to volumes in the low nanoliter range and to thousands to hundreds of thousands of reactions in parallel is necessary to revolutionize processes like early drug discovery.

In this work, we introduce a one-step dip-extraction method that enables the parallel treatment of thousands of droplets with volumes as small as 15 nL without the need for droplet-by-droplet instrumentation on the DMA platform. By immersing the entire DMA into an immiscible organic solvent, such as dichloromethane (DCM), all droplets are simultaneously exposed to a large interfacial area, allowing for substance exchange between the two phases. The strong affinity of the droplets to the hydrophilic surface in combination with the surface tension, ensures droplet integrity throughout the whole process.[18] This instrument-free, scalable, and robust approach allows efficient compound transfer and represents the first general method for solvent-based purification at the nanoliter scale with true parallelization. In addition, this method enables parallel addition of compounds to the nanoliter droplets. It expands the scope of miniaturized chemical workflows on the DMA and offers a critical enabling step for future high-throughput synthesis and screening applications.

2. Results and Discussion

2.1. Method Introduction

A schematic depiction of the dip-extraction method is shown in **Figure 1A**. First, an aqueous solution containing the desired additives is dispensed onto the hydrophilic spots of a droplet microarray. Next, the complete slide is immersed into a suitable organic solvent. The contact between the aqueous droplets and the organic solvent allows the exchange of substances in both directions, depending on their affinity and solubility. After removing

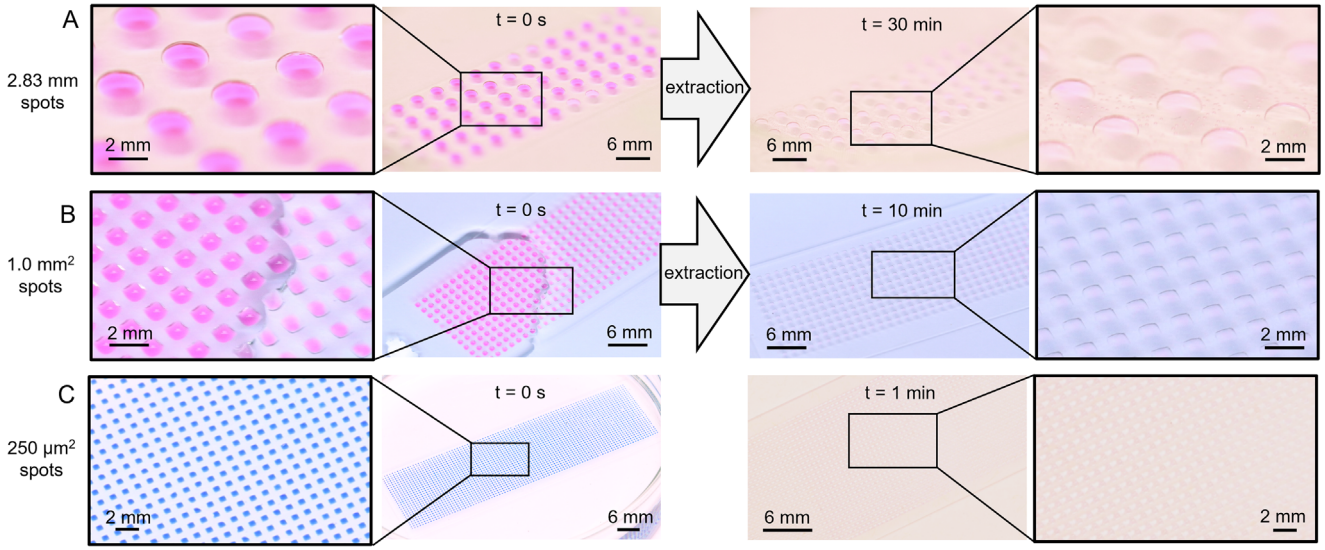

Figure 2. Parallel high-throughput extraction of Rhodamine B from aqueous droplets of different sizes from 5 µL to 15 nL. A) Each spot of a DMA slide containing 80 round spots (2.83 mm diameter) was filled with 5 µL of 0.4 mM aqueous Rhodamine B solution. The slide was immersed in DCM (t = 0 s), and the droplets were extracted until the color of the dye vanished (t = 30 min). Magnifications of the slide images at the beginning and at the end of the extraction are shown for improved visibility. B) Each spot of a DMA slide containing 672 square spots (1.0 mm^2) was filled with 250 nL of 0.4 mM aqueous Rhodamine B solution. The slide was immersed in DCM (t = 0 s), and the droplets were extracted until the color of the dye vanished (t = 10 min). Magnifications of the slide images at the beginning and at the end of the extraction are shown for improved visibility. C) Each spot of a DMA slide containing 2688 square spots (250 μm^2) was filled with 15 nL of either 4.8 mM aqueous Methylene Blue solution or 0.4 mM aqueous Rhodamine B solution. Methylene Blue was used to show droplet stability after immersion (t = 0 s), and Rhodamine B to show the extraction of the dye after short immersion (t = 1 min). Magnifications of the slide images are shown for improved visibility.

the slide from the organic solvent, the aqueous droplets ate still intact, featuring the intended difference. To demonstrate the versatility of the dip-extraction method, we applied it across four distinct use cases that highlight its core functionalities. If the aqueous droplets contain compounds that have a high affinity to the organic phase, they can be removed from the droplets by transferring them into the organic phase (Figure 1B). To parallelly add a substance to all aqueous droplets, the organic phase can be supplemented with the compound before immersing the aqueous droplets (Figure 1C). To seal droplets and prevent them from evaporation during incubation while not changing their composition, the slide can be immersed in an organic solvent that does not extract the compounds contained in the aqueous droplets (Figure 1D). The droplet microarray can also be used as a reaction platform, each spot featuring an independent reaction vessel. After performing the desired reaction in the aqueous droplets, the slide can be immersed in an organic solvent to extract remaining reactants and side products while the product remains in the aqueous phase (Figure 1E). These examples collectively establish dip-extraction as a multifunctional approach for simplifying and scaling key operations in HT, miniaturized workflows.

2.2. Droplet Stability and Compound Removal

To assess droplet stability during immersion and to demonstrate the feasibility of compound extraction from aqueous droplets (Figure 1B), droplet microarrays with hydrophilic spots on a superhydrophobic background were prepared from microscope glass slides as described in the experimental section. The spots were varied in spot size and geometry, particularly round spots with a diameter of 2.83 mm and square spots with an area of 1.0 mm^2 or 250 μm^2. For larger droplets, circular spots are typically used, as they help to maintain droplet stability by minimizing the surface area.[16,18] Square spots are advantageous for small-volume droplets, as they enable higher spot density on the array and therefore maximize the number of experiments that can be performed on a single slide.[32] A 0.4 mM aqueous solution of Rhodamine B was dispensed on each spot of a DMA to form the droplets before immersing the slide into an organic solvent. The hydrophilic functionalization of the spots and the superhydrophobic functionalization of the background ensure the liquid stays on the spot and forms a round droplet. Featuring high solubility for many compounds, DCM is the most common solvent for organic extraction and is therefore also chosen as the organic solvent for this extraction method. Rhodamine B was chosen as a model compound for extraction as it has a decent solubility in water, but similarly to most organic compounds, it preferentially partitions into the organic phase due to its structure containing hydrophobic groups like several aromatic rings and alkyl chains. Therefore, the dye is progressively extracted from the droplets upon contact.

The stability of the droplets and the extraction ability was tested for the larger 2.83 mm diameter spots (**Figure 2A**) as well as the smaller 1.0 mm^2 (Figure 2B) and 250 μm^2 (Figure 2C) spots, showing the slide directly after immersion at t = 0 s and after complete extraction as well as magnified views of both time points for all spot sizes. For the smallest droplets (250 μm^2), visualization of Rhodamine B proved difficult due to the very small volume and rapid extraction. Therefore, methylene blue

Table 1. Water solubility, interfacial tensions, calculated adhesive forces on round 2.83 mm diameter spots, and experimental observation of droplet stability for tested organic solvents and air.

Solvent	Water solubility in % *w/w* [a)]	Interfacial tension γ in mN/m	Adhesive force in µN for 2.83 mm spots	Experimental observation
Air	–	72.8[35]	159	Stable
Dichloromethane	1.7	28.1[35]	61.6	Stable
Chloroform	0.8	31.6[35]	69.2	Stable
Cyclohexane	0.006	50.2[35]	110	Stable
n-Hexane	0.009	51.1[35]	112	Stable
Toluene	0.05	35.4[36]	77.6	Stable
Ethyl Acetate	8.3	6.8[37]	14.9	Unstable
Diethyl Ether	6.9	11.0[35]	24.1	Unstable
n-Butanol	20	1.8[35]	3.94	Unstable

[a)] Values are obtained from NIST Chemistry WebBook, NIST Standard Reference Database Number 69.

(4.8 mM), a dye that remains predominantly in the aqueous phase due to its highly polar structure and ionic nature, was used additionally to show droplet stability after immersion. As for the larger spots, Rhodamine B was applied to check the extraction from the spots. In all cases, droplets maintained their shape and position upon immersion in DCM, demonstrating the mechanical stability of the system. While the smallest spots have already turned colorless shortly after immersion, a progressive loss of color could be observed for the larger droplets: initially, only the droplet periphery lost its pink color, while the core remained colored. Over time, the entire droplet became nearly transparent, confirming efficient transfer of Rhodamine B into the organic phase. The larger the spot size, the longer it took to visually complete the extraction process. This is based on three reasons: First, the larger the droplet volume the more Rhodamine needs to be extracted from each droplet. As the volume is increased by several magnitudes with increasing spot sizes (15 nL for 250 µm^2, 250 nL for 1.0 mm^{2,} and 5 µL for 2.83 mm diameter), this has a high impact on the extraction time. Second, the surface-to-volume ratio is higher for smaller droplets, enabling a faster extraction. Third, the color intensity is not only dependent on the dye concentration, but also on the liquid volume. A slight dye trace is much better visible if the volume of the droplet is higher. Consequently, the concentration of Rhodamine B in the larger droplets needs to be lower for them to be considered colorless. These reasons led to a much longer extraction time of 30 min for the largest spot size.

Nevertheless, it could be shown that the dip-extraction method enables the parallel extraction from multiple droplets in one single step, while preserving droplet integrity, for all tested spot sizes. The number of droplets on one microscope slide measuring 7.60 × 2.50 cm adds up to 80 for 2.83 mm spots, 672 for 1.0 mm^2 spots, and 2688 for 250 µm^2 spots, respectively. If a larger glass slide of Microtiter Plate (MTP)-format (12.8 × 8.55 cm) would be used, the number of spots could be increased to 504 × 2.83 mm diameter spots, 4760 × 1.0 mm^2 spots or 19210 × 250 µm^2 spots when keeping the dot pitches equal. It should also be possible to increase the number of spots by decreasing their size even further, however, special liquid dispensers are needed to apply droplets of volumes below 10 nL homogeneously, and precautions must be made to prevent evaporation during the droplet application and slide transfer.

The dominant force holding a droplet to a spot is the capillary adhesion force $F_{adhesion}$, which can be approximated using the liquid-vapor or lipid-liquid interfacial tension γ, the diameter of the droplet base, and the receding contact angle θ_R.[33] As mercaptoethanol-functionalized surfaces are highly polar, the receding contact angle is approximated as 0°.[34] By calculating the adhesion force and incorporating the water solubility, it can be determined if aqueous droplets remain stable on the DMA when immersed in a specific organic solvent. The water solubility of the tested solvents, calculated adhesive forces for 2.83 mm diameter spots, and the experimental observation if the droplets remain stable when dipped into the organic solvent are given in **Table 1**. The formula used for calculation (Equation S1, Supporting Information), parameters, and calculations for other spot sizes (Table S1, Supporting Information) are given in the Supporting Information. When comparing the calculated adhesive forces with the experimental observations, it clearly shows that droplets do not remain stable if the adhesive force is below 15% of the adhesive force in air. Five out of the eight tested solvents remained adhesive forces between 39 and 70% relative to the value in air, and experiments could prove droplet stability in those cases. Thus, the system does not only works with DCM as an organic solvent, but also with other solvents listed in Table 1, as long as the interfacial tension and therefore the adhesive force are high enough. It also stands out that the three solvents which did not feature droplet stability have a comparatively high water solubility, which can also serve as an indicator if a specific solvent works with the introduced method.

To quantify the extraction efficiency of the dip-extraction method, 250 nL of a 0.4 mM Rhodamine B solution was dispensed onto a DMA with 1.0 mm^2 hydrophilic spots. The slide was immersed in DCM for time intervals ranging from 10 s to 5 min (**Figure 3**A,B). After extraction, the slides were imaged using a document scanner, and droplet color intensities were quantified using the Grid Screener software and normalized to pre-extraction values.[38] Using a calibration curve (Figure S2, Supporting Information), the residual Rhodamine B concentration was determined for each time point. As shown in Figure 3C, Rhodamine B extraction followed an exponential decay, with the most

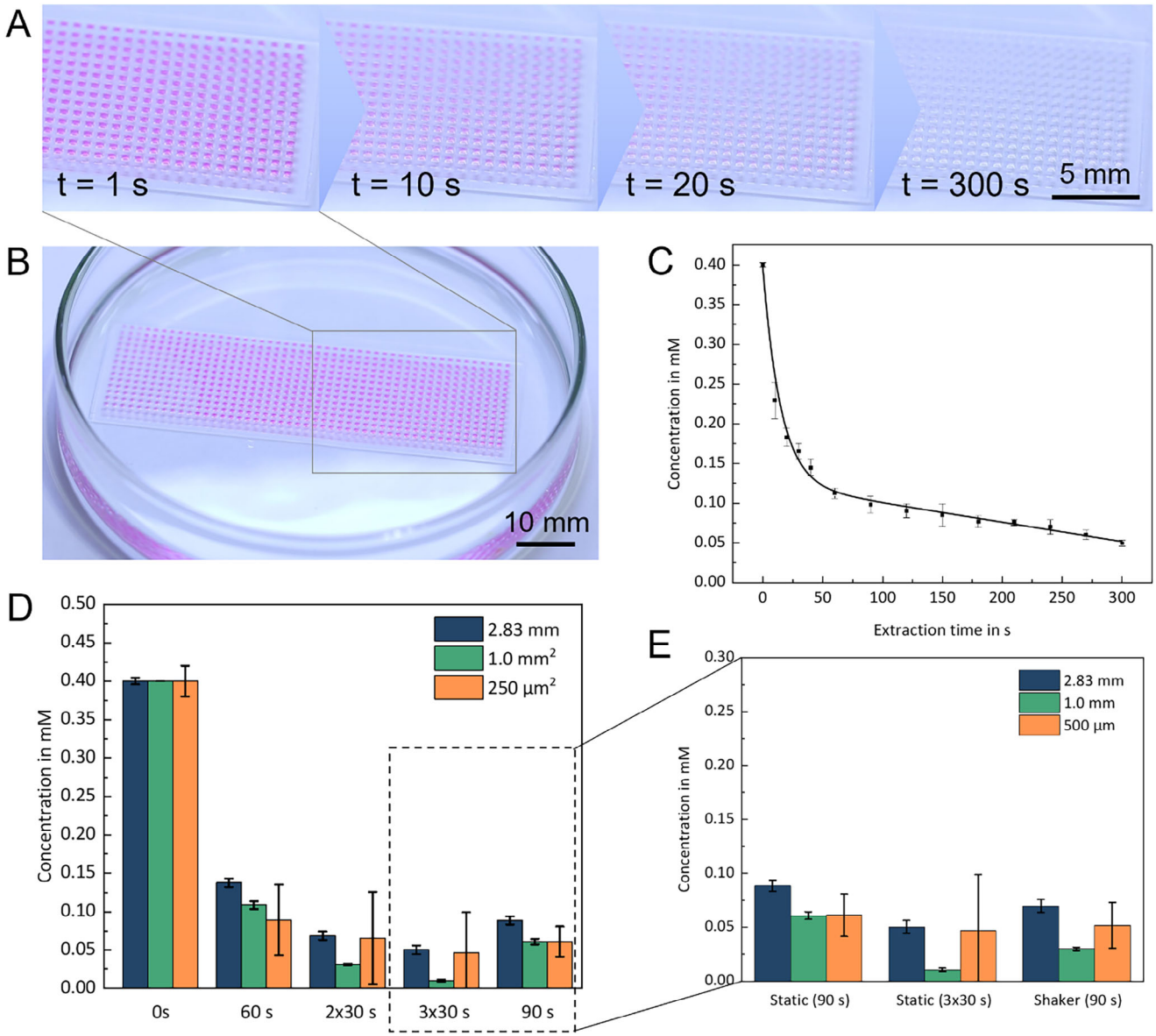

Figure 3. Quantification of the dip-extraction efficiency. A) Section of a slide with 1.0 mm^2 spots containing 250 nL of 0.4 mM aqueous Rhodamine B solution during the immersion in DCM. The corresponding time since immersion is indicated in the pictures. Scale bar measures 5 mm. B) Image of the whole slide with 1.0 mm^2 spots immersed in a petri dish filled with DCM. Scale bar measures 10 mm. C) Concentration of Rhodamine B remaining in the droplets after certain extraction times between 10 s and 5 min. The concentration was calculated from the determined color intensity after extraction using a calibration curve (Figure S3, Supporting Information). An exponential model was fitted to the values, depicted as a solid black line. The equation used was $y = A_1*\exp(-x/t_1) + A_2*\exp(-x/t_2)+ y_0$ with $y_0 = -2194$, $A_1 = 0.2752$, $t_1 = 14.94$, $A_2 = 2194$ and $t_2 = 8.000*10^6$, leading to an R-squared value of 0.9993. Standard deviations are depicted as error bars. D) Concentration of Rhodamine B in droplets on 2.83 mm diameter (blue), 1.0 mm^2 (green), and 250 μm^2 (orange) spot slides before extraction and after certain extraction times. The total extraction times were either 60 s, 60 s with DCM exchange after 30 s, 90 s, or 90 s with DCM exchange every 30 s. The concentration was calculated from the color intensity using calibration curves for each droplet size (Figures S2–S4, Supporting Information). The values were derived from three independent experiments, each containing multiple droplets. Standard deviations are depicted as error bars. E) Comparison of the remining Rhodamine B concentration in the droplets on slides with 2.83 mm diameter (dark blue), 1.0 mm^2 (green) and 250 μm^2 (orange) spots for 90 s extraction time under static conditions, either with DCM exchange every 30 s or in the same DCM for the whole extraction time, or moving on a shaker for 90 s. Standard deviations are depicted as error bars. Each experiment was repeated on three independent DMAs with multiple droplets per repetition.

pronounced decrease occurring within the first 50 s. Beyond this point, the process slowed down, decreasing linearly upon a concentration of 0.05 mM after 5 min, corresponding to an extraction efficiency of ≈90% after a single extraction step.

To further improve this efficiency, we evaluated a strategy commonly used in bulk extractions – multiple extractions with fresh solvent. Slides were sequentially transferred to fresh DCM every 30 s for total extraction durations of 60 or 90 s. Color intensities were again analyzed using Grid Screener software and translated into concentration via calibration curves (Figures S2–S4, Supporting Information).[38] Overall spot sizes, repeated extractions led to improved efficiency compared to static 60 and 90-s extraction (Figure 3D). In all cases, a 60-s extraction with one DCM exchange (2 × 30 s) performed equally well (for 250 μm^2) or even better (for 1.0 mm^2 and 2.83 mm) than a static 90-s extraction. A further improvement could be shown for 2 transfers (3 × 30 s extraction), reducing Rhodamine B concentration to 0.05 mM on 2.83 mm diameter spots and 0.01 mM on 1.0 mm^2 spots, corresponding to total extraction efficiencies of 89% and 98%, respectively. Compared to a static 90-s extraction, the extraction could be improved by ≈7% in both cases using the DCM exchange method. Due to the small droplet volume and, associated therewith, a low color saturation for low Rhodamine B concentration, the concentrations and standard deviations are higher for the small 250 μm^2 spots. Nevertheless, the described trend can be seen.

To explore a more practical alternative to solvent exchange, we tested whether constant agitation enhances extraction equally well. Slides were immersed in DCM and placed on a shaker for 90 s. As shown in Figure 3E, shaking could enhance the extraction efficiency compared to a static 90-s extraction, leading to remaining concentrations of 0.07 mM in droplets on 2.83 mm diameter spots, 0.03 mM on 1.0 mm^2 spots, and 0.05 mM on 250 μm^2 spots. However, the solvent exchange approach remained superior, offering a method for fast extraction even for larger droplet sizes.

Next, we evaluated the selectivity of dip-extraction using Rhodamine B (pink dye), which preferentially partitions into the organic phase, and methylene blue (blue dye), which remains in the aqueous phase. Droplets containing either dye separately or a mixture of both were dispensed onto a DMA with 1.0 mm^2 hydrophilic spots, the latter forming violet droplets due to the color combination (**Figure 4A**). The array was then immersed in DCM for 3 min. As Rhodamine B was extracted into the organic phase, the pink droplets became nearly colorless, while the violet droplets turned blue, retaining only methylene blue (Figure 4B). After extraction, all initially pink droplets lost most of their color, and the former violet and blue droplets became indistinguishable, confirming the selective removal of Rhodamine B (Figure 4C). To quantify these changes, color intensities of all droplets were measured before and after extraction using the Grid Screener software (Figure 4D).[38] The pink droplets retained only 20% of their initial intensity, while the intensity of blue droplets remained nearly unchanged. In the case of violet droplets, separate measurements of pink and blue intensity before and after extraction revealed a drop in pink intensity from 60% to 16%, aligning with the values observed for pure Rhodamine B droplets (Figure 4E). Simultaneously, the blue intensity increased to 83%, approaching the levels of pure methylene blue droplets, further confirming selective extraction.

To assess cross-contamination, Rhodamine B solution and pure water were alternately pipetted onto a DMA with 2.83 mm spots (Figure 4F). The array was then immersed in DCM for 30 min, and droplet color intensities were measured before and after extraction (Figure 4G).[38] While Rhodamine B droplets exhibited a significant decrease in color intensity, confirming successful extraction, water droplets showed no detectable pink coloration (<1%), demonstrating that no cross-contamination occurred between neighboring spots.

To further demonstrate the versatility of dip-extraction, we evaluated its performance on patterned areas with significantly larger volumes. Specifically, a slide featuring a Karlsruhe Institute of Technology (KIT) logo pattern was fabricated, and each compartment was filled with 10–30 μL of a 0.4 mM Rhodamine B solution, depending on the compartment size (**Figure 5A**). The slide was then immersed in DCM, and the solvent was exchanged every 2 min to accelerate the extraction. Complete removal of Rhodamine B was achieved after 20 min (Figure 5B). A visual depiction of the extraction process is shown in Figure 5C. As expected, due to the larger volumes used compared to previous experiments with smaller droplets, the extraction required a longer duration and multiple solvent exchanges. Nevertheless, the process remained effective, confirming the scalability of dip-extraction to macroscopic patterns.

Having established the functionality and robustness of our method, we next compare it to alternative solvent-extraction strategies reported in the literature. Surface nanodroplets formed via solvent exchange have been extensively studied for nanoextraction and related applications.[28–30] While these systems offer good control at the femtoliter scale, they often rely on complex formation dynamics, solvent-exchange protocols, or microfluidic flows, which can limit throughput and general usability. In contrast, our approach operates at the nanoliter to microliter scale, using pre-formed droplets on a patterned substrate. This allows for parallel extraction over hundreds of discrete droplets with no requirement for flow control, surfactant stabilization, or reaction chamber sealing. Regarding the extraction kinetics and efficiency, surface nanodroplet-based methods achieve near complete extraction within seconds to a few minutes.[27] In addition to the flow-enhanced transfer, the droplets also have a very high surface-to-volume ratio due to their very small volumes in the femtoliter scale, accelerating the extraction.[28–29] In contrast, our system relies on passive diffusion, which is slower and requires manual solvent exchange to accelerate the process. Due to the fast analyte transfer, surface nanodroplets are better suited for sensing and analyte preconcentration, while our method is advantageous for on-chip synthesis, post-reaction purification, and screening applications where easier volume adjustments and simpler workflows are required. Additionally, our method only requires minimal equipment, while nanodroplet-based methods usually need precise flow cells. Besides solvent-exchange-based surface nanodroplet platforms, other DMA-compatible strategies have been reported for reagent delivery and purification. Benz et al. introduced a droplet sandwiching method, where reagent transfer occurs by direct vertical contact between two aligned slides containing discrete droplets.[19] While this approach enables rapid one-step exchange, it requires precise alignment and is limited

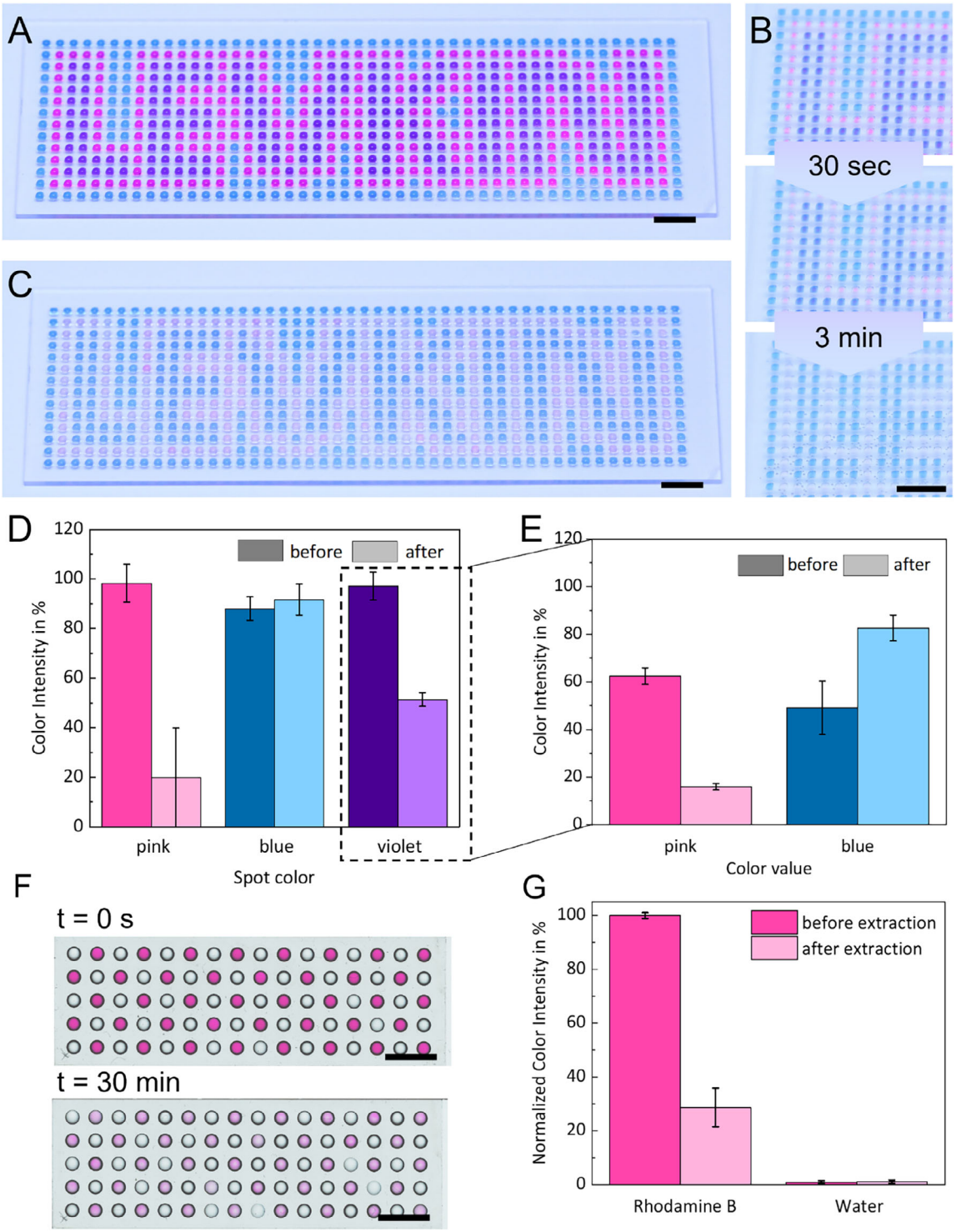

Figure 4. Selective separation of two dyes from 250 nL droplets on 1.0 mm^2 droplets and cross-contamination test using 5 µL droplets on 2.83 mm droplets. A) A pattern was dispensed containing aqueous droplets with either 0.40 mM Rhodamine B, 0.23 mM Methylene Blue, or a 1:1 mixture of 0.40 mM Rhodamine B and 0.44 mM Methylene Blue. Scale bar measures 5 mm. B) Pictures of the slide during the immersion process. Extraction was performed in static mode. The further the extraction, the more colorless the pink spots become, and the bluer the violet spots become. Scale bar measures 5 mm. C) Slide after 3 min immersion in DCM. Scale bar measures 5 mm. D) Color intensity of pink, blue, and violet droplets before (dark) and after (light) the extraction. E) Separation of the color values of violet droplets into intensity of blue and pink before (dark) and after (light) the extraction. F) Cross-contamination test on a slide with 2.83 mm spots. 5 µL of water or 5 µL of 0.4 mM Rhodamine B solution were pipetted on the spots alternating. The slide was scanned before and after 30 min static extraction in DCM. Scale bars measure 10 mm. G) Normalized color intensity of water and Rhodamine B before and after 30 min extraction in DCM. Values were received from scans shown in F).

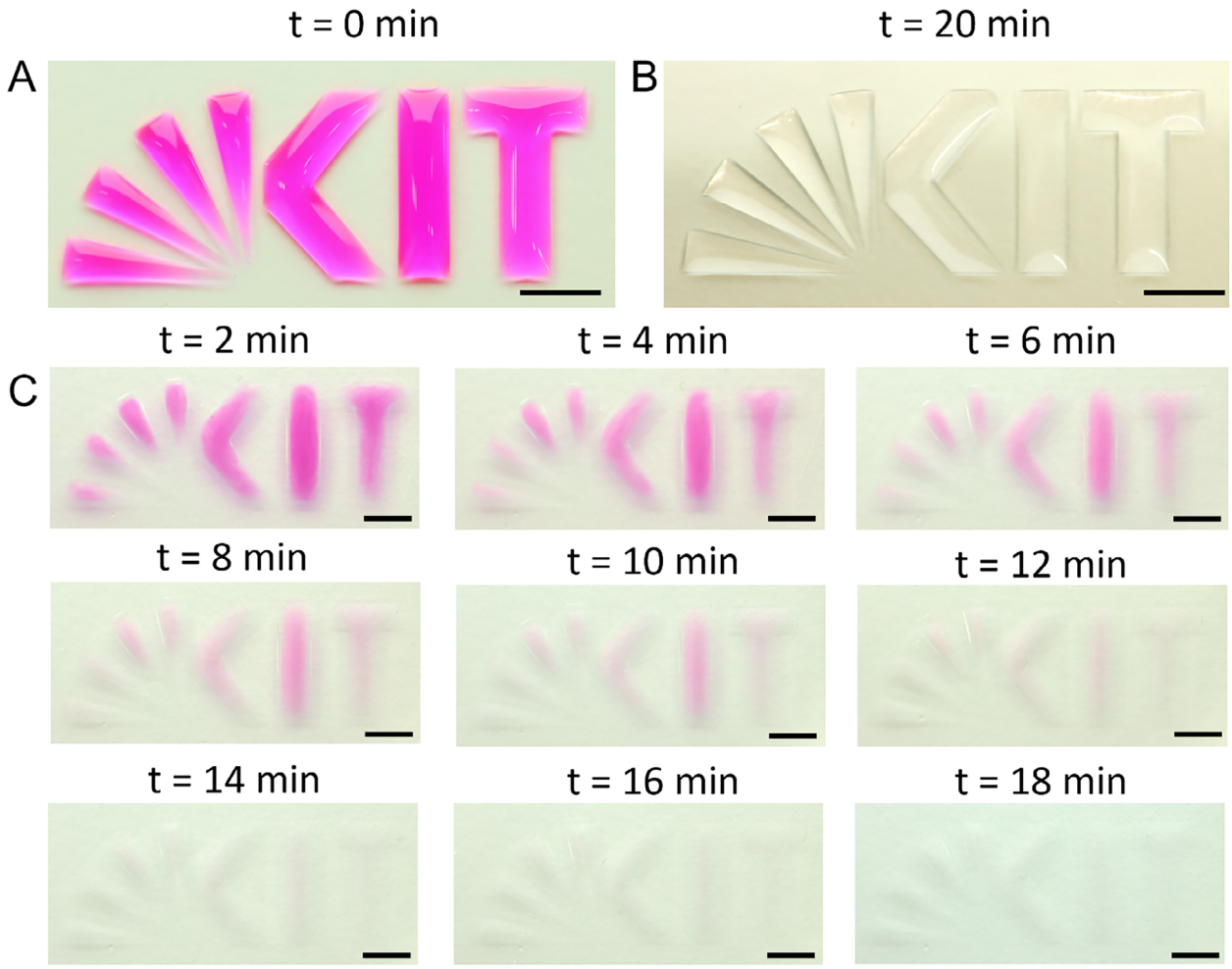

Figure 5. Dip-extraction of a pattern with a larger area. A pattern was filled with 0.4 mM Rhodamine B solution and extracted by immersion in DCM. A) Slide before extraction. B) Slide after 20 min extraction with DCM. To accelerate the extraction, DCM was exchanged every 2 min. C) Extraction process of the pattern during immersion in DCM. A picture was taken every 2 min until complete extraction. All scale bars measure 5 mm.

to larger droplet volumes as the process is prone to droplet deformation and merging instability at smaller scales. Wiedmann et al. later developed a horizontal droplet-merging method on the DMA by placing immiscible droplets side by side and performing the extraction between droplets on the same slide.[31] This simplifies alignment, but still depends on accurate dispensers and is limited to droplets of ≈100 nL or larger. In contrast, our dip-extraction method eliminates the need for droplet-by-droplet instrumentation or mechanical contact, enabling robust compound delivery and extraction in volumes between 5 µL and 15 nL. These characteristics make our approach uniquely suited for highly miniaturized and scalable chemical workflows.

2.3. Parallel Compound Addition

A closely related application of dip-extraction is the addition of a substance to aqueous droplets via the organic phase (Figure 1C). This is achieved by dissolving a compound in DCM, followed by immersion of the droplet-containing slide, allowing diffusion into the aqueous phase. To demonstrate this principle, aqueous droplets of three different pH values (acidic, neutral, basic) were dispensed onto a DMA and immersed in DCM containing bromothymol blue (**Figure 6**A,B). This pH indicator appears blue in basic solutions (pH > 7.6), yellow under acidic conditions (pH < 6.0), and green in between.[39] Immediately after immersion, the basic droplets turned blue, the neutral droplets appeared turquoise, and the acidic ones remained colorless. Over time, the color intensity increased, with neutral droplets turning green after 15 s (Figure 6C). After 2 min, the slide was removed from the DCM (Figure 6D,E). While the basic droplets remained blue and the acidic ones turned slightly yellow, the neutral droplets unexpectedly became bright yellow instead of green. This deviation likely results from bromothymol blue acting as a weak acid, shifting the pH in small-volume droplets.[39] To minimize this effect, the experiment was repeated using larger 2.83 mm spots, where the droplet volume is greater. In this case, the droplets developed the expected colors after 2 min, confirming successful substance transfer without significant pH shifts (Figure 6F). This approach enables the parallel delivery of compounds into thousands of droplets within seconds using a single immersion step. For example, pH-based colorimetry on DMA could be used to screen

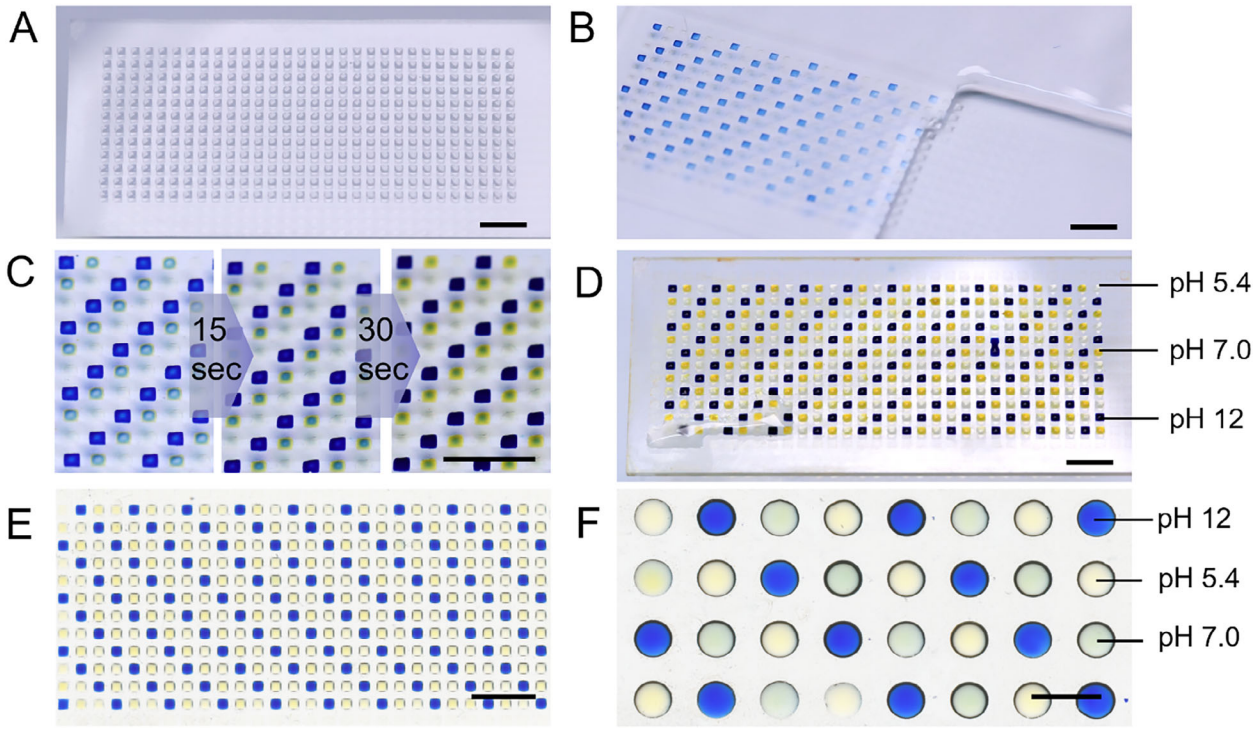

Figure 6. Parallel addition of a chemical to hundreds of droplets in a single step without any pipetting steps. A) 150 nL of aqueous solutions with three different pH values (5.4, 7.0, 12) were applied on a DMA with 1.0 mm^2 spots. B) Slide during immersion in DCM containing bromothymol blue. The droplets turn colorful directly after immersion. C) Zoomed region of the slide after immersion for specific times. D) The slide was taken out after 2 min of immersion. E) Scanned image of a slide with 1.0 mm^2 spots after 30 s staining. F) Scanned image of a slide with 2.83 mm diameter round spots containing 3 µL aqueous droplets with different pH values per spot after staining in DCM containing bromothymol blue for 2 min. All scale bars measure 10 mm.

for enzyme activity in a miniaturized setting, where enzymatic conversion shifts the local pH. Similarly, the addition of weakly basic or acidic drugs could be tracked by changes in pH-sensitive dyes. In chemical sensing, this method could help identify acidic or basic impurities. Advantageous over other methods, it avoids the need for pipetting and allows real-time optical readout across hundreds of discrete assays. Compared to a conventional 384-well plate assay, the dip-extraction method significantly reduces both reagent consumption and handling time. In a standard assay using 25 µL per well, a 384-condition screen would require ≈10 mL of primary reagent. By contrast, using 200 nL droplets on a DMA requires only ≈77 µL of the same reagent, which represents over 98% reduction in reagent cost. The cheaper second reagent is then delivered to all conditions in a single dip-extraction step instead of dispensing 384 individual additions, reducing the assay setup time from at least 30 min to under 5 min. These efficiencies make the dip-extraction method highly suitable for applications mentioned above.

2.4. Evaporation Prevention and Synthesis Purification

Building on the high stability of aqueous droplets on the DMA (demonstrated in Figure 2), submersion in an organic solvent can also serve as a simple and effective method to prevent droplet evaporation by creating a protective liquid layer above them (Figure 1D). This approach is particularly valuable for long-term incubations, where evaporation threatens experimental integrity in miniaturized systems.[32] To demonstrate this effect, 250 nL droplets of water supplemented with methylene blue for enhanced visibility were dispensed onto 1.0 mm^2 DMA spots (**Figure** 7A). Instead of DCM, cyclohexane (cHex) was chosen as the organic solvent for incubation. As depicted in Table 1, cHex has a water solubility of only 0.006%, which is significantly lower than the one of dichloromethane with 1.7%. Thus, cyclohexane can prevent aqueous droplets from evaporating for a longer time without slowly reducing the volume of the droplets by dissolving the water. After a total incubation time of 5 days, all the droplets were still intact. This simple immersion-based sealing method provides a low-cost alternative to conventional humidity chambers or oil overlays, offering a scalable solution for prolonged droplet-based assays and high-throughput screening applications.[40,41]

Purifying reaction products at the microliter scale poses a significant challenge, as standard bulk purification methods such as washing, liquid-liquid extraction, or column chromatography are not feasible.[31,42] By utilizing the DMA as a reaction platform, our dip-extraction method enables one-step purification of all droplets simultaneously, offering a high-throughput solution for miniaturized synthesis (Figure 1E). To demonstrate this concept, we performed the base-catalyzed ester hydrolysis of butyl acetate (Figure 7B) on the DMA. The workflow is depicted in Figure 7C. A solution containing 4.3 mg mL^{-1} butyl acetate and 4.0 mg mL^{-1} sodium hydroxide (NaOH) was prepared in

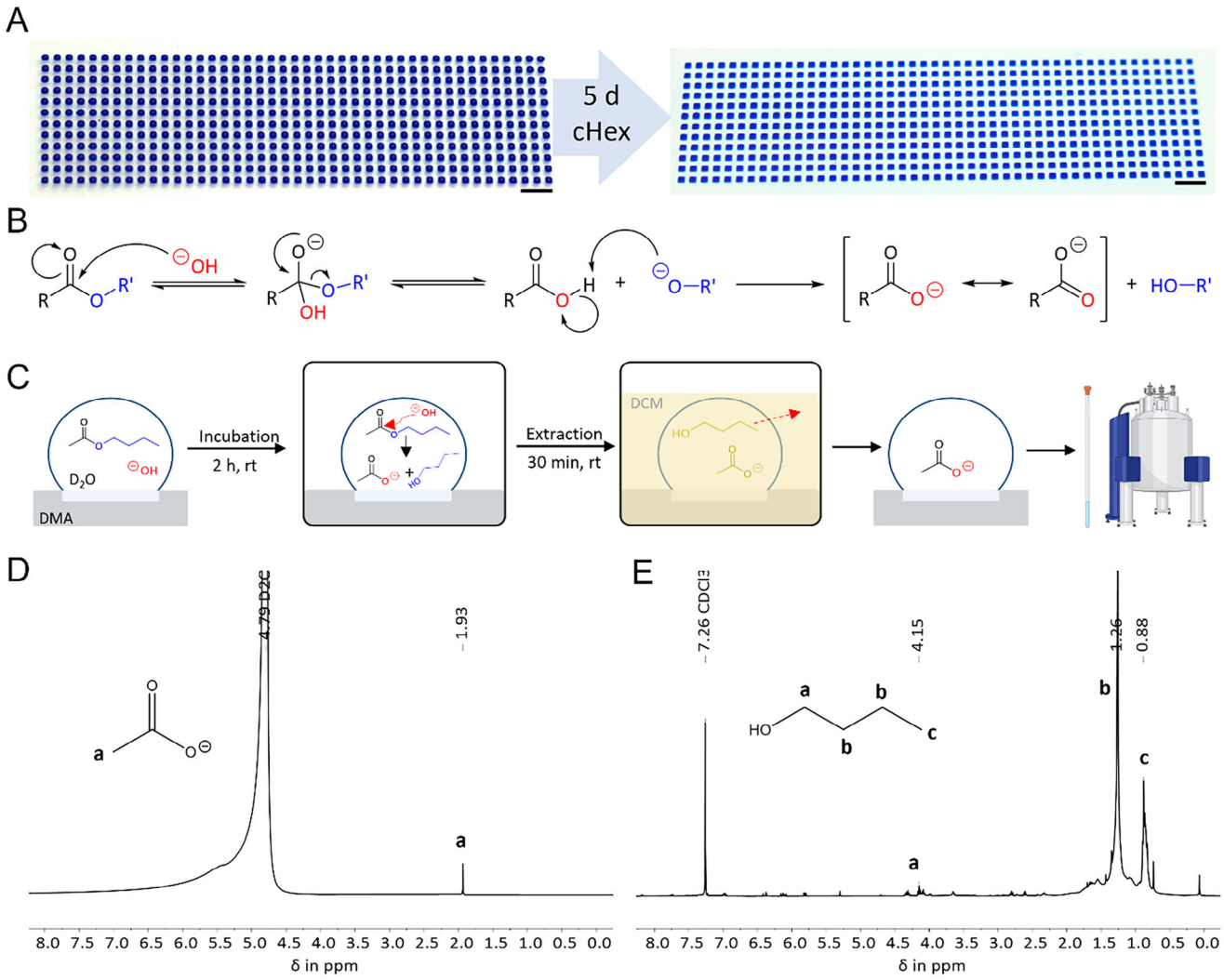

Figure 7. Evaporation prevention of 250 nL droplets on 1.0 mm^2 spots and ester hydrolysis and purification of droplets with 4 µL volume on 2.83 mm round spots. A) To show the ability of the system to prevent evaporation, 250 nL of a 4.85 mM methylene blue solution was printed on each spot of a 1.0 mm^2 spot. The slide was immersed in cyclohexane for 5 days. After the incubation time, all spots were still intact. B) General mechanism of base-catalyzed hydrolysis of esters. The hydroxy anion $^{-}$OH (red) is added to the carbonyl carbon before eliminating the alkoxide $^{-}$OR' (blue). In the subsequent step, the proton of the generated carboxylic acid is transferred to the alkoxide, yielding the alcohol HOR' and the resonance-stabilized carboxylate ion, which is less electrophilic than the carboxylic acid and cannot be attacked anymore, making the reaction irreversible. C) Workflow of ester hydrolysis and purification on DMA. A solution containing 4.3 mg mL^{-1} butyl acetate and 4.0 mg mL^{-1} sodium hydroxide in deuterium oxide was pipetted on the spots. The droplets were incubated for 2 h at room temperature under humid conditions to allow the basic ester hydrolysis to proceed, resulting in acetic acid and butan-1-ol. After incubation, the slide was completely immersed in DCM for 30 min for purification. Due to its higher solubility in DCM, butan-1-ol is extracted while acetic acid remains in the droplets. D) ^{1}H-NMR of the droplets after reaction and extraction. The peak at 1.93 ppm is assigned to the CH_3-group of acetic acid. E) ^{1}H-NMR of the DCM used for extraction. The multiplet at 4.15 ppm is assigned to the HO-CH_2-group of butan-1-ol, the peak at 1.26 ppm is assigned to the other CH_2-groups of butan-1-ol, the peak at 0.88 ppm to the CH_3-group, respectively.

deuterium oxide (D_2O) instead of water to facilitate nuclear magnetic resonance (NMR) analysis of reaction products. 4 µL of this solution was dispensed onto each spot of a 2.83 mm DMA, and the slide was incubated at room temperature for 2 h to allow the reaction to proceed, resulting in acetic acid and butan-1-ol. For purification, the DMA was immersed in DCM for 30 min. Due to their different affinity, deprotonated acetic acid remained in the aqueous droplets, while butan-1-ol was extracted into the DCM phase. NMR analysis confirmed successful separation of the products: The NMR spectrum of the aqueous droplets (Figure 7D) displayed a single peak at 1.93 ppm, corresponding to the methyl group of acetic acid.[43] Conversely, the NMR spectrum of the organic residue (Figure 7E) revealed three distinct peaks at 0.88, 1.26, and 4.15 ppm assigned to the CH_3- and CH_2-groups of butan-1-ol, respectively.[44]

Compared to conventional bulk-phase purification, our method reduces solvent consumption by more than 50-fold. In standard workflows, each reaction is typically purified individually via three liquid-liquid extraction steps, consuming at least 30 mL of solvent per reaction. In contrast, our

dip-extraction method purifies all reactions on a DMA slide simultaneously using just 40 mL of DCM in total. For a slide containing 80 reactions, this corresponds to only 500 µL of solvent per reaction, exemplifying a dramatic reduction in both volume and waste. In addition, miniaturization of the reactions inherently reduces reagent costs. Beyond material savings, dip-extraction also offers substantial time efficiency. While purifying 80 bulk reactions individually would require ≈20 h, all reactions on the DMA can be purified in parallel within 30 min.

The base-catalyzed ester hydrolysis of butyl acetate was selected as a model reaction because it meets the two essential criteria for successful dip-extraction. First, all reagents must be soluble in the aqueous phase to ensure homogeneous reaction conditions. Second, the desired product must preferentially remain in the aqueous droplets, while side products and unreacted reagents partition into the organic phase. In this case, the deprotonated acetic acid product remains in the aqueous phase, while butan-1-ol is efficiently extracted into the DCM layer. When both conditions are met, the method offers a simple and effective strategy for purifying reactions directly on the droplet microarray and can be extended to more complicated reactions at the microscale. By eliminating the need for complex liquid handling, dip-extraction significantly expands the utility of miniaturized reaction platforms. Furthermore, it can simplify workflows like biological screenings of structurally new drugs as all steps from synthesis of up to thousands of structurally different molecules on one slide, over purification to biological screening, can be performed on the same platform without transferring the compound of interest.

3. Conclusion

Our method introduces a single-step, rapid, scalable, parallel, and high-throughput approach for liquid manipulation in miniaturized systems. With a single dipping step, this method enables selective removal or addition of substances, efficient purification of chemical reactions without complex pipetting steps, and effective evaporation protection—overcoming long-standing challenges in droplet-based processing. The method supports a wide range of droplet geometries and volumes down to 15 nL. Such small volumes enable the parallel processing of 2688 samples on a microscope glass slide or over 19 000 on an MTP-sized glass slide. For this scale and throughput, there are to date, basically no easily performable methods for purification, parallel addition or extraction. In this study, we used a liquid dispenser to generate arrays of aqueous droplets, however, this can also be done using simpler alternatives, such as dipping the patterned slide into an aqueous solution or rolling a droplet across the surface, which eliminates the need for expensive equipment entirely.[16,45] As increasing throughput while reducing volumes is essential in many areas of research, such as synthesis, diagnostics, and screenings, to save costs and reduce workload, our method opens new possibilities to simplify miniaturized workflows and even broaden the possible applications. Especially workflows like drug development, where a biological assay follows the combinatorial synthesis of a molecule library, can be simplified, as the new method in combination with the DMA, allows the execution of the whole workflow from synthesis of thousands of compounds on one slide, over purification to biological screening on one platform. Recent advances in bioengineering, such as HT single-cell metabolomics platforms (Cao et al., 2024) and 3D-bioprinted scaffolds for bioactive vesicle delivery (Li et al., 2024) highlight the growing need for parallelized substance delivery and rapid functional screening methods.[46–47] The dip-extraction approach introduced here could serve as a versatile addition to such platforms, enabling rapid and uniform introduction of compounds into microdroplets, for example, to add reagents for analysis or to perform colorimetric assays to quickly achieve preliminary results.

While the method offers a step forward, certain limitations remain. The choice of compatible solvents is restricted to solvents with low water solubility and high interfacial tensions to ensure droplet stability. Depending on the droplet composition, the stability of the droplets can also be negatively influenced. For instance, the addition of organic surfactants can reduce the surface tension of water as they disrupt the cohesive hydrogen bonding between water molecules at the surface. Similarly, the addition of acidic or basic compounds can alter surface charge interactions with the substrate, leading to reduced droplet stability. However, if the concentration of the surfactant is not too high, stability can be maintained by reducing the droplet volume or by choosing an organic solvent like cyclohexane in which droplets maintain a higher interfacial tension. Future developments will focus on integration of this method into lab-on-chip technologies and microscale reaction engineering – transforming dip-extraction into a foundational tool for high-throughput and miniaturized reactions and screenings.

4. Experimental Section

Materials and Chemicals: Nexterion Glass B microscope glass slides were obtained from Schott Technical Glass Solutions GmbH (Jena, Germany). Photomasks were bought from Rose Fotomasken (Bergisch Gladbach, Germany). Acetone, ethanol, 2-propanol, and DCM were used in technical grade without further purification from Merck KGaA (Darmstadt, Germany). Triethoxyvinylsilane, 1*H*,1*H*,2*H*,2*H*-perfluorodecanethiol (PFDT), and Rhodamine B were obtained from Sigma–Aldrich (Darmstadt, Germany). Bromothymol blue and hydrochloric acid were purchased from VWR International GmbH (Darmstadt, Germany), and Aerosil 200 silica nanoparticles were purchased from Evonik Industries AG (Essen, Germany). Methylene blue hydrate was purchased from Honeywell (Offenbach, Germany). All chemicals were used without further purification.

Preparation of Patterned DMA Slides: The nanoparticle solution for coating the slides was prepared by mixing 250 mg Silica nanoparticles with 30 mL ethanol, followed by 30 min sonication at room temperature with an Elmasonic S 30 H sonicator. 340 µL vinyltrimethoxysilane and 200 µL concentrated hydrochloric acid were added and sonicated for 60 min. The solution was aged at room temperature overnight. The glass slides were activated by 10 min UV treatment using a UVO-cleaner 42–220 from Jelight Company Inc. (California, USA). The slides were spin-coated for five times by applying 500 µL of the nanoparticle solution and spinning at 1000 rpm for 15 sec with a SPIN150i spin coater (SPS Europe, Ingolstadt, Germany). After that, the slides were cured for 1 h at 150 °C with a heating plate Präzitherm PZ60 (Harry Gestigheim GmbH, Düsseldorf, Germany). The slides were washed with acetone and patterned by using 250 µL of a 10% (v/v) PFDT solution in isopropanol and a photomask covering the required spots. The slides were irradiated for 90 s with UV light in a UVA cube (Dr. Hönle AG, Gilching, Germany) and washed with acetone. In the last step, 250 µL of a solution containing 10 % (v/v) 2-mercaptoethanol in ethanol/water (1:1) was added, the slide was covered with a quartz glass, and irradiated again for 90 s. Depending on the photomask, the spot sizes

compromised 2.83 mm diameter (5 × 16 = 80 spots), 1.00 mm side length (14 × 48 = 672 spots) or 500 µm side length (28 × 96 = 2688 spots).

Dispensing on DMA Slides: For all dispensing steps, Certus Flex from Fritz Gyger AG (Gwatt, Switzerland) was used. The DMA slides were placed in a slide holder purchased from Aquarray (Eggenstein–Leopoldshafen, Germany). The solutions were dispensed with the respective calibration at 0.3 bar.

Extraction Procedure: In the dipping experiments, DMA slides prepared according to the described protocol were used. If not stated otherwise, the pattern was filled with 0.4 mM aqueous Rhodamine B solution (2.83 mm round: 5 µL, 1.0 mm^2: 250 nL, 250 μm^2: 15 nL). For volumes of 4 µL or more, an Eppendorf pipette Xplorer plus was used. If the desired volume was smaller than 4 µL, it was dispensed with a liquid dispenser as described above. All stated droplet volumes refer to the volume dispensed for the droplet formation. Then, the slide was carefully immersed in 45 mL DCM either in a 50 mL centrifuge tube or a 15 cm diameter glass petri dish. After the extraction was done or at a certain time point, the slide was slowly taken out using tweezers. The remaining DCM was dropping off or evaporated within 20 s. The slide was imaged either with a camera or a scanner for further analysis.

Imaging: Photos for visualization were taken with a Canon EOS 90D from Canon Deutschland GmbH (Krefeld, Germany) with a Canon EF 100 mm lens from Canon Deutschland GmbH (Krefeld, Germany). Images for further analysis were taken with a document scanner, CanoScan 8800F from Canon Deutschland GmbH (Krefeld, Germany) at 70% exposure. The images are shown in the figures without any color modification.

Evaluation via Grid Screener: For color intensity evaluations, the Grid Screener tool was used for automated image analysis, as detailed in[38] First, the DMA array layout was identified and re-centered, and the spot size and geometry were defined. Subsequently, the color intensity of each spot was automatically analyzed based on the RGB values of the color of interest. The resulting intensities were provided as spot-wise values and further analyzed according to the experiment protocol. If not stated otherwise, the average of all spots was calculated, excluding the outer rows in case of 1.0 mm^2 spots and the outer two rows in case of 250 μm^2 to minimize evaporation effects.

Graphics: Graphics were created with BioRender.com.

Supporting Information

Supporting Information is available from the Wiley Online Library or from the author.

Acknowledgements

M.J.I. and J.J.W. contributed equally to this work. This project was partly supported through the Deutsche Forschungsgemeinschaft (DFG) (Heisenbergprofessur project number 406232485, LE 2936/9-1). Furthermore, the authors thank the Helmholtz Program "Materials Systems Engineering" for the support.

Open access funding enabled and organized by Projekt DEAL.

Conflict of Interest

The authors declare no conflict of interest.

Data Availability Statement

The data that support the findings of this study are available from the corresponding author upon reasonable request.

Keywords

droplet microarrays, high-throughput, liquid-liquid extractions, miniaturization, purifications

Received: May 23, 2025
Revised: July 18, 2025
Published online:

[1] G. M. Whitesides, *Nature* **2006**, *442*, 368.
[2] N. Shembekar, H. Hu, D. Eustace, C. A. Merten, *Cell Rep.* **2018**, *22*, 2206.
[3] J. C. Love, J. L. Ronan, G. M. Grotenbreg, A. G. van der Veen, H. L. Ploegh, *Nat. Biotechnol.* **2006**, *24*, 703.
[4] S. Vyawahare, A. D. Griffiths, C. A. Merten, *Chem. Biol.* **2010**, *17*, 1052.
[5] M. Y. Mayday, L. M. Khan, E. D. Chow, M. S. Zinter, J. L. DeRisi, *PLoS One* **2019**, *14*, 0206194.
[6] J. J. Agresti, E. Antipov, A. R. Abate, K. Ahn, A. C. Rowat, J.-C. Baret, M. Marquez, A. M. Klibanov, A. D. Griffiths, D. A. Weitz, *Proc. Natl. Acad. Sci. USA* **2010**, *107*, 4004.
[7] Y. Tian, M. Seifermann, L. Bauer, C. Luchena, J. J. Wiedmann, S. Schmidt, A. Geisel, S. Afonin, J. Höpfner, M. Brehm, X. Liu, C. Hopf, A. A. Popova, P. A. Levkin, *Small* **2024**, *20*, 2307215.
[8] W. Zheng, N. Thorne, J. C. McKew, *Drug Discovery Today* **2013**, *18*, 1067.
[9] X. D. Xiang, *Annu. Rev. Mater. Sci.* **1999**, *29*, 149.
[10] M. Mondal, A. K. Hirsch, *Chem. Soc. Rev.* **2015**, *44*, 2455.
[11] D. B. Weibel, W. R. Diluzio, G. M. Whitesides, *Nat. Rev. Microbiol.* **2007**, *5*, 209.
[12] P. S. Dittrich, A. Manz, *Nat. Rev. Drug Discovery* **2006**, *5*, 210.
[13] D. Mark, S. Haeberle, G. Roth, F. von Stetten, R. Zengerle, *Chem. Soc. Rev.* **2010**, *39*, 1153.
[14] M. Jones, R. L. Goodyear, *ACS Med. Chem. Lett.* **2023**, *14*, 916.
[15] S. Y. Teh, R. Lin, L. H. Hung, A. P. Lee, *Lab Chip* **2008**, *8*, 198.
[16] W. Feng, E. Ueda, P. A. Levkin, *Adv. Mater.* **2018**, *30*, 1706111.
[17] G. E. Jogia, T. Tronser, A. A. Popova, P. A. Levkin, *Microarrays* **2016**, *5*, 28.
[18] A. A. Popova, K. Demir, T. G. Hartanto, E. Schmitt, P. A. Levkin, *RSC Adv.* **2016**, *6*, 38263.
[19] M. Benz, M. R. Molla, A. Boser, A. Rosenfeld, P. A. Levkin, *Nat. Commun.* **2019**, *10*, 2879.
[20] A. Rosenfeld, P. A. Levkin, *Adv. Biosyst.* **2019**, *3*, 1800293.
[21] A. A. Popova, M. Reischl, D. Kazenmaier, H. Cui, T. Amberger, P. A. Levkin, *SLAS Technol.* **2022**, *27*, 44.
[22] R. A. Houghten, *Proc. Natl. Acad. Sci. U. S. A.* **1985**, *82*, 5131.
[23] N. Cankarova, E. Schutznerova, V. Krchnak, *Chem. Rev.* **2019**, *119*, 12089.
[24] A. M. Garcia, N. Jung, C. Gil, M. Nieger, S. Bräse, *RSC Adv.* **2015**, *5*, 65540.
[25] S. L. Schreiber, *Science* **2000**, *287*, 1964.
[26] M. Li, L. Bao, H. Yu, X. Zhang, *J. Phys. Chem. C* **2018**, *122*, 8647.
[27] J. Qian, G. F. Arends, X. Zhang, *Langmuir* **2019**, *35*, 12583.
[28] Z. Wei, M. Li, H. Zeng, X. Zhang, *Anal. Chem.* **2020**, *92*, 12442.
[29] M. Li, B. Dyett, H. Yu, V. Bansal, X. Zhang, *Small* **2019**, *15*, 1804683.
[30] J. B. You, D. Lohse, X. Zhang, *Lab Chip* **2021**, *21*, 2574.
[31] J. J. Wiedmann, Y. N. Demirdögen, S. Schmidt, M. A. Kuzina, Y. Wu, F. Wang, B. Nestler, C. Hopf, P. A. Levkin, *Small* **2023**, *19*, 2204512.
[32] Y. Wu, J. E. Urrutia Gomez, H. Zhang, F. Wang, P. A. Levkin, A. A. Popova, B. Nestler, *Droplet* **2024**, *3*, 115.
[33] D. W. Pilat, P. Papadopoulos, D. Schaffel, D. Vollmer, R. Berger, H. J. Butt, *Langmuir* **2012**, *28*, 16812.
[34] B. A. Johnson, J. Kreuter, G. Zografi, *Colloids Surf.* **1986**, *17*, 325.
[35] G. M. Kontogeorgis, S. Kill, *Introduction to Applied Colloid and Surface Chemistry*, John Wiley & Sons, Chicester **2016**.
[36] H. M. Backes, J. J. Ma, E. Bender, G. Maurer, *Chem. Eng. Sci.* **1990**, *45*, 275.

[37] H. Yoon, M. Oostrom, C. J. Werth, *Environ. Sci. Technol.* **1993**, *43*, 2318.
[38] M. P. Schilling, S. Schmelzer, J. E. U. Gomez, A. A. Popova, P. A. Levkin, M. Reischl, *IEEE Access* **2021**, *9*, 166027.
[39] A. Avdeef, *ADMET DMPK* **2023**, *11*, 419.
[40] C. Li, Z. Hite, J. W. Warrick, J. Li, S. H. Geller, V. G. Trantow, M. N. McClean, D. J. Beebe, *Sci. Adv.* **2020**, *6*, aay9919.
[41] E. Berthier, J. Warrick, H. Yu, D. J. Beebe, *Lab Chip* **2008**, *8*, 852.
[42] A. Rios, T. S. Holloway, P. H. Chao, C. De Caro, C. C. Okoro, R. M. van Dam, *Sci. Rep.* **2022**, *12*, 10263.
[43] H. E. Gottlieb, V. Kotlyar, A. Nudelman, *J. Org. Chem.* **1997**, *62*, 7512.
[44] L. Van Lokeren, G. Maheut, F. Ribot, V. Escax, I. Verbruggen, C. Sanchez, J. C. Martins, M. Biesemans, R. Willem, *Chemistry* **2007**, *13*, 6957.
[45] L. Shi, S. Liu, X. Li, X. Huang, H. Luo, Q. Bai, Z. Li, L. Wang, X. Du, C. Jiang, S. Liu, C. Li, *Mikrochim. Acta* **2023**, *190*, 260.
[46] J. Cao, Q. J. Yao, J. Wu, X. Chen, L. Huang, W. Liu, K. Qian, J.-J. Wan, B. O. Zhou, *Cell Metab.* **2024**, *36*, 209.
[47] X. R. Li, Q. S. Deng, P. L. Liu, S. H. He, Y. Gao, Z. Y. Wei, C.-R. Zhang, F. Wang, X.-Q. Dou, H. Dawes, S.-C. Guo, S.-C. Tao, *View* **2024**, *5*, 20230069.